JCTC Journal of Chemical Theory and Computation

ARTICLE

pubs.acs.org/JCTC

The Influence of Cholesterol on the Properties and Permeability of Hypericin Derivatives in Lipid Membranes

Emma S. E. Eriksson and Leif A. Eriksson*

School of Chemistry, National University of Ireland—Galway, Galway, Ireland

Supporting Information

ABSTRACT: The promising photosensitizing properties of hypericin, a natural quinine substituted with hydroxyl and alkyl groups, have led to the proposal that it can be utilized in photodynamic therapy. Neither the detailed mechanism behind the powerful action of hypericin, arising as a result of light excitation, nor the intracellular localization and transportation of the molecule is yet fully understood. The behavior of hypericin derivatives in a pure dipalmitoylphosphatidylcholine (DPPC) lipid membrane has recently been studied theoretically by means of molecular dynamics simulations. Natural membranes however contain many important constituents—cholesterol being one of the most essential—that influence the function and structure of the membrane, and thereby also the behavior of drug molecules therein. In the present study, we investigated hypericin and its brominated derivatives in membranes containing 9 and 25 mol % cholesterol. The results show that the presence of cholesterol in the membrane affects the permeability of the hypericin molecules and does so differently for the various molecules in the two membranes. Hypericin containing one bromine was found to exhibit the lowest free energy profile for the transport process into the lipids, and also the highest permeability coefficients, indicating that this molecule displays the fastest and easiest diffusion in the membranes. All three molecules were found to accumulate most preferably close to the polar headgroup region in both membranes.

1. INTRODUCTION

1.1. Cholesterol in Lipid Membranes. Cholesterol (Figure 1) is an important compound in nature, possessing many essential properties, not only as precursor to several vitamins and hormones but also as an important constituent in biological membranes, besides phospholipids and glycolipids, in which it for example increases mechanical strength, regulates phase behavior, and reduces the passive permeability of water and other small molecules. The cholesterol molecule is made up of three groups that have all proven essential for their effect on membranes: the fused rigid steroid rings, the hydroxyl group attached to one of the rings, and the short flexible hydrocarbon chain.[1] Although intracellular synthesis of cholesterol takes place in the endoplasmic reticulum (ER) and external cholesterol is transported to the lysosomes where it is hydrolyzed, the majority of the cellular cholesterol is found in the plasma membrane,[2] and an equilibrium process in which cholesterol is being transported between the cell membrane and the cytosol has been proposed.[3]

Cholesterol is found in a wide range of concentrations in various animal membranes, normally around 20−30 mol %, but plasma membranes of some cells contain up to 50 mol %.[4] In membranes in which the cholesterol concentration is high (>25 mol %), an additional phase exists besides the solid-ordered and liquid-disordered ones: the liquid-ordered phase.[5,6] In this phase, the lipids are translationally disordered and conformationally ordered, i.e., a combination of the two other phases in which the lipids are either completely ordered or disordered. In the liquid-ordered state, both ordering[7,8] and condensing[9,10] effects caused by cholesterol are observed. Cholesterol has also been extensively studied in the controversial field of lipid rafts and its presence in those. Lipid rafts are dynamic liquid-ordered domains made up by cholesterol, sphingolipids, and proteins important in, for example, signaling.[11]

1.2. Computational Studies of Cholesterol-Containing Membranes. Basic initial computational studies of cholesterol/lipid membranes were performed more than two decades ago[12−14] and have been followed by numerous more extended and detailed studies carried out by Monte Carlo (MC) and molecular dynamics (MD) simulation techniques in recent years. The improvement of computers and algorithms has enabled progression to study larger systems, including more than 1000 lipids, and the use of longer simulation time scales.[15,16] Many properties of cholesterol-containing membranes as seen experimentally have been reproduced theoretically, thereby also enabling the evaluation of detailed properties that are difficult to observe experimentally.

It has been clearly shown, both experimentally and theoretically, that cholesterol has a crucial effect on the properties of the membrane and that the cholesterol concentration plays an important role. A wide range of concentrations of cholesterol has been included in the computational studies to cover for the occurrence in natural membranes. Cholesterol has an ordering and condensing effect, two features that are closely related and that have been observed in numerous computational studies at varying cholesterol concentrations.[15−22] The ordering and condensing effect results in a decreased membrane surface area and thereby a reduced area per lipid. Chui et al. performed simulations of DPPC bilayers with cholesterol concentrations ranging from 4 to 50 mol % and found a linear relationship between

Received: September 15, 2010
Published: January 28, 2011

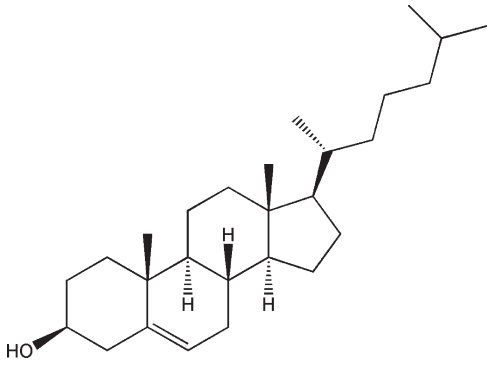

Figure 1. Chemical structure of the cholesterol molecule.

increased cholesterol concentration and a decrease in area per lipid at cholesterol concentrations in the range of 12−50 mol %.[21] However, Tu et al. showed that a cholesterol concentration of 12.5 mol % had no significant effect on the conformation and packing of the hydrocarbon chains.[23] Smondyrev and Berkowitz observed that the cholesterol molecules exhibit a larger tilt when the concentration is low, whereas at higher concentrations, in which the hydrocarbon tails are more ordered and extended, cholesterol displays a reduced tilt.[17] A reduction in electron density in the center of the DPPC bilayer was also observed with higher cholesterol concentrations as well as an increase in hydrophobic thickness,[17] supported by neutron-scattering experiments on DMPC bilayers.[24]

Martinez-Seara et al. recently published a detailed study of the unique structural functionality of cholesterol in its ability to initiate the liquid-ordered phase.[25] They showed that, at concentrations below ∼30 mol %, the cholesterol molecules avoid locations adjacent to each other but prefer locations separated by ∼1 nm, i.e., located in the second coordination shell. It was also found that triangular connections between neighboring cholesterol molecules exist, as opposed to demethylated cholesterol (missing the two off-plane methyl groups; Dchol) for which linear connections exist. The two faces of cholesterol were also studied in detail, and it was shown that ordering and condensing was less pronounced in membranes with Dchol, indicating that the off-plane methyl groups were essential for the unique properties of cholesterol.[26]

Overall, unsaturated lipids show weaker interaction with cholesterol than saturated ones, and condensation and ordering is consequently less evident.[27] Solvation of saturated lipid chains occurs most preferably with the smooth α face of cholesterol, the flat side with no substituents.[20] In lipids containing one saturated and one unsaturated chain, cholesterol is preferably solvated by the saturated acyl chain.[28] For unsaturated chains, however, the β face induces higher ordering.[27] Even lipid chains not neighboring any cholesterol in the system[20] or within a radius of at least a few nanometers[28] were found to display higher order than in a pure lipid bilayer. The position of the double bond in unsaturated lipids has been shown to significantly influence the interactions with cholesterol regarding condensing and ordering, with the double bond located in the middle of the lipid acyl chain resulting in the smallest effects, whereas when located at the end of the chain, it resulted in larger effects.[29,30]

Niemelä et al. recently used three large membrane systems (1024 lipids in each) with varying unsaturated palmitoyloleoylphosphatidylcholine (POPC), palmitoylsphingomyelin, and cholesterol composition in order to study lipid rafts.[16] Two of the systems represented membranes with coexistent liquid-ordered and liquid-disordered domains as a result of high cholesterol content. They confirmed that the raft domain membranes most likely influence the function of membrane proteins, mainly due to significant differences in pressure profiles compared to the liquid-disordered single phase membrane.

Water molecules penetrate deeper into the bilayer interior in cholesterol-containing membranes and can therefore form hydrogen bonds with the hydroxyl group of cholesterol.[19] The number of possible hydrogen bonds also depends on the depth at which cholesterol is located, and this in turn depends on the lipid composition in the bilayer. In a DPPC bilayer, the cholesterol molecules are located deeper into the lipid interior than in a DMPC bilayer, and the number of hydrogen bonds with water is consequently reduced in the DPPC membrane.[18,26] At low cholesterol concentrations, the number of hydrogen bonds with water is lower than at higher concentrations, as a result of the cholesterol molecules being able to locate deeper inside the DPPC bilayer.[17] Pure saturated lipid membranes are however not frequently found in nature; membranes are usually composed of mixtures of different lipids, unsaturated ones being more common than saturated, and other components. However, pure saturated lipid membranes are commonly utilized as computational models mainly due to a lack of experimental data for unsaturated lipids, which make parametrization a difficult issue. The fact that most lipids have at least one saturated chain also makes the choice of saturated lipids useful. It is however worth emphasizing that the computational studies discussed herein were performed using different programs, force fields, and lipid compositions. These differences can slightly influence the results.

1.3. Permeation of Molecules in Cholesterol-Containing Membranes. Cholesterol was shown to reduce the permeability of ions and small molecules such as Na^+, K^+, Cl^-, and glucose through lipid membranes.[31] It was also discovered that the permeability of water is reduced in cholesterol-containing membranes and that this depends on the cholesterol concentration.[32]

There are only a few studies performed on the unique behavior of drug molecules in lipid membranes containing cholesterol, as most of the theoretical and experimental focus has been directed into studying the effect of cholesterol itself on various lipid membranes. An experimental study performed on model membranes showed that cholesterol decreases the permeability of large drug molecules mainly due to the condensing effect of cholesterol on the membrane.[33] This condensation may in particular affect large and rigid drug molecules. Molecular interactions between the drug molecule and cholesterol can also delay the permeation through the membrane, such as has been shown for small nonsteroidal anti-inflammatory drugs.[34] Several studies have confirmed that cholesterol strongly influences the interactions between peptides (drugs as well as endogenous compounds) and the membrane.[35−38]

Drug interactions with cholesterol are important also because of the fact that many drugs are transported in the body by liposomes and lipoproteins. Liposomes are commonly used in the drug delivery of both hydrophilic and hydrophobic drugs, as they contain an aqueous core surrounded by a circled lipid bilayer that can contain a significant amount of cholesterol. Hydrophobic drugs that are administered into the bloodstream can bind to lipoproteins, which are the natural cholesterol transporters in the body, and can, in those, interact with the cholesterol molecules.

With the use of computational methods making it possible to reproduce many of the features of cholesterol in membranes, the behavior of small molecules such as drugs in these can be studied

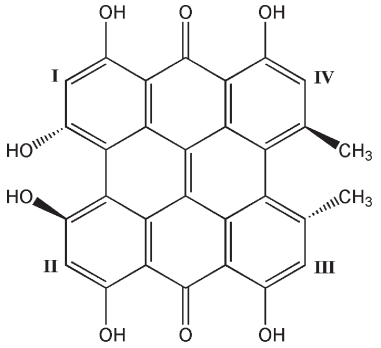

Figure 2. The hypericin molecule with numbers indicating where bromine substitution was modeled (I, Hy-Br; I−IV, Hy-4Br).

as well. Such studies can promote the design of drugs with desirable properties.

1.4. Hypericin. We have in a recent study investigated the behavior of the potent photodynamic drug hypericin (Hy; Figure 2) with no, one (Hy-Br; position I, Figure 2), and four bromines (Hy-4Br; positions I−IV, Figure 2) in a pure DPPC bilayer using molecular dynamics simulations.[39]

Hypericin is a natural compound found in the *Hypericum* species, whose advantageous medical properties have been known for several thousand years. Besides the well-known antidepressive properties of *Hypericum* extracts,[40] it has been found that hypericin possesses antiviral[41−46] and antitumor[47−50] properties, as a result of the formation of reactive oxygen species (ROS) such as singlet oxygen upon light excitation, indicating that the compound could be used in photodynamic therapy (PDT). Hypericin has also been successful in the field of photophysical diagnosis of early stage tumors, as it accumulates specifically in tumor tissue from which the fluorescence of the drug can be detected.[51−53]

The interest in making the hypericin molecule a more effective photodynamic drug has led to modifications such as halogenation. Bromination of hypericin increases the formation of ROS due to enhanced intersystem crossing from the first excited singlet state to the triplet state[54,55] and has shown potential phototoxic activity against viruses.[56] Hypericin has been found in various cell compartments; however, the exact cellular target as well as the transport into the cell and its action of cell destruction is still to be elucidated. However, there seems to be a preference for hypericin to accumulate in lipid membranes due to its hydrophobic character, where it can initiate lipid peroxidation.[57,58]

In a recently published study, it was proposed that cholesterol is the major reason why hypericin selectively accumulates in lipid membranes.[59] A high amount of hypericin was found to localize in raft domains rich in cholesterol rather than in less ordered regions rich in lipids. The emission spectrum suggests interactions between cholesterol and the π electrons of hypericin, resulting in effective packing of the two molecules due to the common planar structure. These results indicate that hypericin most likely can enter the cell membrane through diffusion; however, in the presence of lipoproteins such as low-density lipoproteins in the blood, these can be likely carriers of hypericin and can also assist in cell-entering.[60−62] Lipoproteins, as the natural carriers of cholesterol in the body, are in that sense important in the aspect of possible cholesterol interactions with the drug.

In our previous molecular dynamics study of hypericin derivatives in pure DPPC lipid bilayers, we found a strong preference for the hypericin molecules to accumulate in the bilayer, close to the polar headgroups and the interface between the lipids and water, a location that enables interactions between the hydroxyl groups of hypericin and water.[39] The largest gain in free energy for the transfer process of moving from water into the lipids as well as the fastest diffusion through the membrane was shown for Hy-Br, indicating that this molecule would have the highest probability to penetrate the membrane and reach the interior of the cell. Experimentally, it has been shown that halogenated drugs display larger permeability coefficients through lipid membranes.[63]

In order to extend the previous study, we are herein including cholesterol in the membrane model. The study was performed on two cholesterol/lipid membrane systems, one containing a low concentration (9 mol %) cholesterol and one containing a higher concentration (25 mol %) cholesterol, and with the same hypericin derivatives as in the previous study (Hy, Hy-Br, and Hy-4Br; Figure 2). The present study was performed using a membrane model containing twice as many lipids and with twice as long production runs compared to the previous one.

2. COMPUTATIONAL METHODOLOGY

The molecular dynamics program GROMACS (version 4.0.4)[64] was used throughout the study, together with the united atom GROMACS force field. The membrane model used was a dipalmitoylphosphatidylcholine (DPPC) bilayer consisting of 128 lipids and 3655 water molecules that had been equilibrated[65] and simulated for 100 ns.[66−68] This membrane model contains a larger number of lipids than the model used in our previous study; however the number of water molecules is more or less the same, leading to a thinner water phase in the present model.

The cholesterol structure was first geometry optimized using the Gaussian program[69] at the B3LYP/6-31G(d,p) level of theory. Using the coordinates obtained in the quantum optimizations, the topology of the cholesterol molecule was obtained using the PRODRG software[70] through its Web server [http://davapc1.bioch.dundee.ac.uk/prodrg/], which generates topologies based on the GROMOS87 force field. Mulliken charges obtained from the optimization were assigned to the cholesterol molecule, and small charge groups with total charges close to zero were used. Thereafter, the structure was minimized by the steepest descent algorithm followed by a 100 ps equilibration simulation with a time step of 0.5 fs.

Two cholesterol/DPPC bilayers were constructed, one with 9 mol % (cholesterol/lipid ratio 12:116) and one with 25 mol % (cholesterol/lipid ratio 32:96) cholesterol, by randomly replacing lipid molecules with cholesterol in the membrane model. The same number of lipids was replaced in each monolayer. The membranes were minimized using steepest descent and equilibrated for 5 ns at 100 K. A simulated annealing simulation was then performed to increase the temperature from 100 to 500 K and then reduce it to 323 K, in steps of 50 K and 100 ps. The two membranes were equilibrated 20 ns at 323 K.

During the initial simulated annealing of the cholesterol/DPPC systems, the structures and conformations of the membranes were seriously disrupted and the increase in kinetic energy resulting from the heating generated the lipids in a highly flexible disordered state. This led to the possibility for the cholesterol molecules to move around in the membrane, both within and in-between the monolayers. In the membrane containing 32 cholesterol molecules (25 mol %), with initially 16 in each

monolayer, some cholesterol molecules moved in-between the monolayers, resulting in 14 cholesterol molecules in one monolayer and 18 in the other. In the system with 9 mol % cholesterol, the 12 cholesterol molecules stayed in their respective monolayers (six in each) during all simulations.

The geometries of the hypericin molecules were generated as outlined above for cholesterol and the topologies obtained using the PRODRG software. Mulliken atomic charges obtained from the geometry optimizations, as well as small charge groups, were assigned to the molecules. As bromine is not parametrized in the GROMOS87 force field, Lennard-Jones and ligand parameters for chlorine were used instead. For the DPPC phospholipids, a standard united atom force field was applied,[71] and for water, we used the SPC model.[72] Parameters used for the cholesterol and hypericin molecules are provided in the Supporting Information.

Six independent simulations were performed, one for each neutral hypericin derivative (Hy, Hy-Br, and Hy-4Br) in each of the two membranes. Two hypericin molecules of each derivative were inserted into the membrane model, one in the outer region of the water phase and one in the middle of the lipid phase. The systems were equilibrated for 200 ns, followed by 100 ns production runs in which the system trajectories were collected every 0.8 ps. During the equilibrations, the hypericin molecules moved into the lipids at different stages of the simulations. All simulations were performed using a time step of 2 fs. In a set of test simulations, 10 hypericin (Hy only) molecules were also studied in the two membranes. All 10 molecules were initially inserted into the water phase, and the behavior of the molecules was monitored.

In all simulations, the isothermal−isobaric ensemble (NPT) at T = 323 K and p = 1 bar was used. The temperature and pressure were held constant using a Nosé−Hoover thermostat[73,74] with a coupling constant of 0.1 ps and a semi-isotropic Parrinello−Rahman barostat[75,76] with a coupling constant of 1 ps. A particle mesh Ewald scheme[77,78] was used to calculate the electrostatic interactions with a 10 Å cutoff for the real space. The same cutoff was used for van der Waals interactions (Lennard-Jones terms). Bond lengths were constrained using the LINCS algorithm.[79] Analyses were performed on the equilibration runs to verify equilibration convergence and on the production runs from which all reported data were obtained.

A potential of mean force formalism was used to calculate free energy profiles for hypericin molecules across the lipid bilayer (the direction of the z axis). The z component of the force, F_z, acting on the molecule at certain constrained distances between the molecule and the bilayer (DPPC) center of mass was collected at different positions along the z axis. The free energy for the transfer process between z_i and z_f is written as

$$\Delta G = G_{z_f} - G_{z_i} = -\int_{z_i}^{z_f} \langle F_z \rangle_z \, dz \qquad (1)$$

where the bracket means an average over the forces collected at each constrained distance. To calculate the free energy profile for the translocation of each molecule, 34 constrained simulations were performed in which the hypericin molecule was located at positions differing by 0.1 nm along the z axis direction. The starting points for the simulations were sampled from the previous nonconstrained simulations. To sample the points in the middle of the bilayer, where the molecules were never located during the unconstrained simulations, a weak force was used to push the molecule toward the bilayer middle, choosing the value of the force so as to make the least perturbation possible on the bilayer system.

At each point in water (9 mol % cholesterol: 2.8−3.3 nm from the bilayer center; 25 mol % cholesterol: 3.1−3.3 nm from the bilayer center) equilibration was performed for at least 3 ns, followed by a production run of 4 ns. Inside the lipid bilayer (9 mol % cholesterol: 0−2.7 nm from the bilayer center; 25 mol % cholesterol: 0−3.0 nm from the bilayer center), an increase in the sampling was needed due to the slower motion of the molecules, and therefore, each point was equilibrated for at least 4.7 ns and a production run of 10 ns followed. For some of the systems with the hypericin molecules located within or close to the headgroup region, it was difficult to reach an equilibrated system due to competing interactions with the hypericins from the lipids and water. The thinner water phase in the present membrane model reduces the number of constrained simulations as the maximum distance to the bilayer center used herein was 3.3 nm, compared to 4.0 nm in our previous pure DPPC study. In the more condensed 25 mol % cholesterol membrane, the water phase is thicker than in the lower cholesterol membrane (as discussed below), and additional frames further out into the water phase could in principle have been included. However, in order to compare the results from the two membranes, the same number of frames was employed for both systems. The constrained simulations in the 25 mol % cholesterol membrane were run with the z box length fixed, whereas for the 10 mol % cholesterol membrane, this was not possible.

The force acting on the hypericin center of mass was collected at every time step during the production run. A SHAKE algorithm[80] was used to constrain the distance between the center of mass of the bilayer and the hypericin molecules (the molecules were constrained in the z direction but allowed to rotate). In the 25 mol % cholesterol membrane, in which the two monolayers contained different numbers of cholesterol molecules, the constrained hypericin molecule was located in the monolayer containing the most cholesterol (18).

The permeability is defined as the current density divided by the concentration gradient across the membrane. The procedure developed by Marrink and Berendsen[81] was adopted to calculate the permeability coefficients, based on the fluctuation dissipation theorem and using the deviation of the instantaneous force, $F(z,t)$, from the average force acting on the molecule obtained during the constrained dynamics:

$$\Delta F(z,t) = F(z,t) - \langle F(z,t) \rangle \qquad (2)$$

The local time-dependent friction coefficient, ξ, can be calculated from the following autocorrelation function:

$$\xi(z,t) = \langle \Delta F(z,t) \Delta F(z,0) \rangle / RT \qquad (3)$$

where T is the absolute temperature and R is the gas constant. By integrating the friction coefficient, one can obtain the diffusion coefficient, D:

$$D(z) = RT/\xi(z) = (RT)^2 / \int_0^\infty \langle \Delta F(z,t) \Delta F(z,0) \rangle \, dt \qquad (4)$$

This function was fitted to a double exponential using a nonlinear fitting procedure[81] in order to integrate the autocorrelation of the force fluctuations:

$$C(t) = A_0 \exp(-t/\tau_0) + A_1 \exp(-t/\tau_1) \qquad (5)$$

This translates to the molecules moving inside the lipid bilayer on two distinct time scales, corresponding to the two decay times τ_0 and τ_1, one fast and one slow.

The permeability coefficient, P, can be calculated by integrating over the local resistances across the membrane, $R(z)$. $R(z)$ is obtained by dividing the exponential of the previously calculated free energies, $\Delta G(z)$, by the diffusion coefficients, $D(z)$:

$$1/P = \int R(z)\, dz = \int_{z_i}^{z_f} \frac{\exp(\Delta G(z)/kT)}{D(z)}\, dz \qquad (6)$$

Interaction between cholesterol molecules at the two concentrations and for each different hypericin system was monitored through radial distribution functions (RDF), as were interaction between cholesterol and DPPC molecules. The data reveal that the concentration of cholesterol in the current systems is too low for the cholesterols to interact directly—instead they all form a first and even a second coordination shell of DPPC molecules, before the nearest cholesterol molecule appears (COM distances around 1 nm)—in agreement with the findings of Martinez-Seara et al.[25] No specific effects from the different hypericins were observed. The RDFs are provided in the Supporting Information.

3. RESULTS

The fact that cholesterol molecules were exchanged between the monolayers in the 25 mol % cholesterol bilayer during the simulated annealing is an interesting observation. Flip-flopping of cholesterol is an important natural process and has experimentally been demonstrated to occur with a half-time of <1 s.[82] Coarse-grained MD simulations estimated the rate of possible flip-flops to be in the same range.[83] Umbrella sampling MD simulations and atomistic MD simulations have also been applied to study possible flip-flopping of cholesterol.[84] The most probable flip-flop path for cholesterol was calculated with a modified string method and was found to involve the cholesterol molecule first tilting and then moving to the bilayer center. The free energy barrier for the flip-flop in the DPPC bilayer was found to be higher than in diarachidonylphosphatidylcholine (DAPC), but lower than in POPC. However, spontaneous flip-flops of cholesterol have not yet been observed during MD simulation "production runs", although for ketosterol this phenomenon has been detected in atomistic MD simulations.[85] Note that the flip-flops observed in the present study occurred during the simulated annealing, in which the temperature was significantly higher than under normal conditions, resulting in more movement in the system that gives rise to a possible exchange of molecules between the monolayers. No spontaneous flip-flops were observed during the simulations at constant temperature (323 K).

In Figure 3, we show snapshots from the production simulations of the two membranes with hypericin. In the membrane with 9 mol % cholesterol, the lipid and cholesterol molecules are free to move to a larger extent, and the molecules are tilted more than in the bilayer with higher cholesterol content. The hydrocarbon tails of both the lipids and the cholesterol molecules are in a disordered state. The condensing effect of cholesterol is clearly seen in the 25 mol % cholesterol membrane, and the hydrocarbon tails of the lipids and the cholesterol molecules are more ordered and more aligned to the bilayer normal. The increased thickness of the water phase, as a result of the decreased membrane surface area, is also clearly visible in the 25 mol %

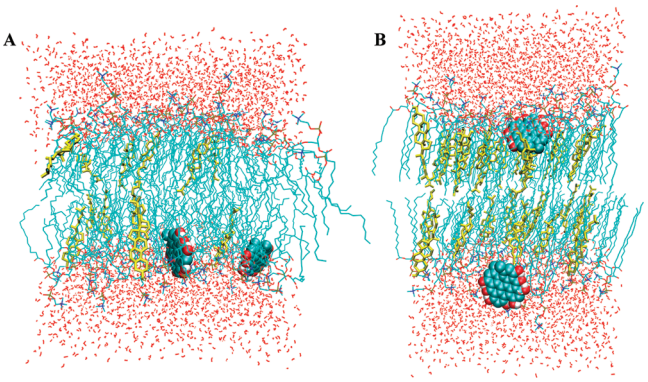

Figure 3. Snapshots from the simulations of two hypericin molecules in (A) 9 mol % and (B) 25 mol % cholesterol membranes. Cholesterol molecules are displayed in yellow.

cholesterol membrane. The condensing effect is due to the smaller size of a cholesterol molecule relative to DPPC, and consequently, with higher cholesterol content, the effect is more pronounced. The cholesterol molecule is shorter than a DPPC molecule and can therefore fit tightly in-between two DPPC molecules, often with its hydroxyl group in the level of the carbonyl group of the DPPC molecules. The condensing effect can also be displayed as the area per lipid, which decreases with an increasing concentration of cholesterol. The area per DPPC lipid was calculated by subtracting from the total area per monolayer the total area occupied by cholesterol molecules and dividing the difference by the number of lipids in one monolayer. We used the area per cholesterol molecule (=32 Å^2) obtained from X-ray diffraction experiments,[86] assuming that the cholesterol area remained constant, whereas the area per lipid was taken as an average over the last 10 ns of the equilibration of the membranes. For the 9 mol % cholesterol membrane, the area per lipid was estimated to be 59.7 Å^2 and, in the 25 mol % cholesterol membrane, 48.1 Å^2 in the monolayer with 18 cholesterol molecules and 50.8 Å^2 in the monolayer with 14 cholesterol molecules. Smondyrev and Berkowitz used the same approach to calculate the area per lipid in membranes with 11 and 50 mol % cholesterol, giving 58.3 Å^2 and 44.7/46.5 Å^2, respectively.[17] In a pure DPPC membrane, the average area per lipid has been measured to be 61.6 Å^2.[87] Our generated data thus fit well into this range.

The hypericin molecules entered the membranes at different stages of the equilibration simulations. However, the same equilibration time (200 ns) was used for all six systems, and by that time all of the molecules were well inside the lipids. During the equilibrations, the molecules were free to enter any of the two monolayers, from the water or from the center of the bilayer. In the case of Hy in the 9 mol % cholesterol membrane and Hy-4Br in the 25 mol % cholesterol membrane, the two molecules ended up in the same monolayer. However, the molecules were not interacting, as the minimum distance between the two molecules during the production runs was overall larger than the van der Waals cutoff of 10 Å. Neither of the hypericin molecules crossed the center of the bilayer or returned into the water phase after entering the monolayer region.

In the 9 mol % cholesterol membrane, all three hypericin derivatives entered the lipids in regions where the local cholesterol concentration was low. The reason for this behavior might be that the local density is lower in the regions where there are no

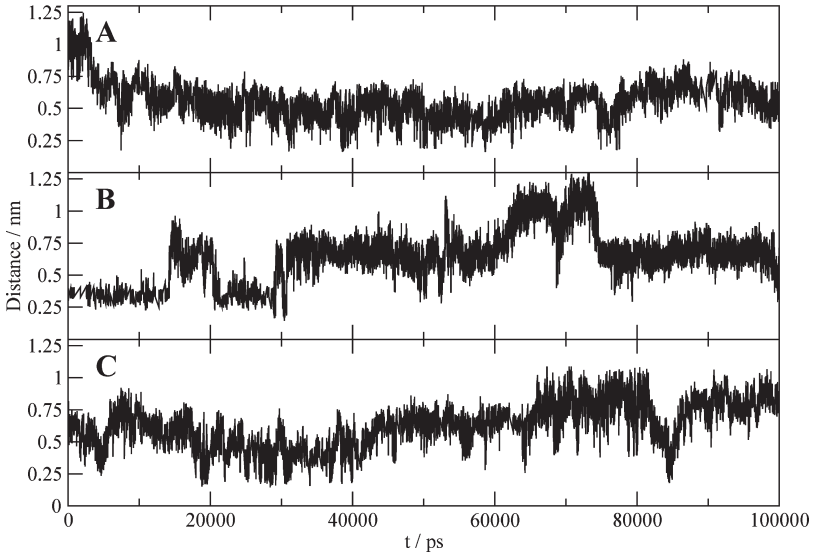

Figure 4. Minimum distance (nm) between any pair of atoms of a hypericin molecule (A, Hy; B, Hy-Br; C, Hy-4Br) and a cholesterol molecule during the production simulations in the 9 mol % cholesterol membrane.

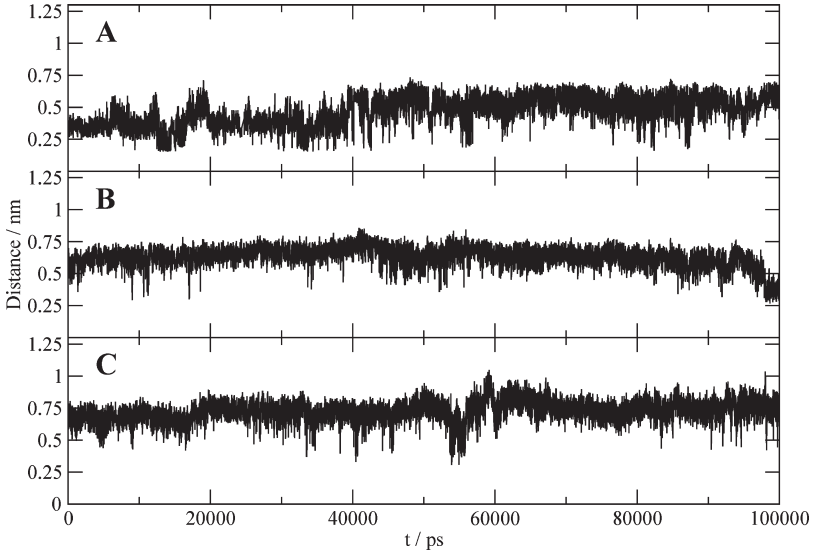

Figure 5. Minimum distance (nm) between any pair of atoms of a hypericin molecule (A, Hy; B, Hy-Br; C, Hy-4Br) and a cholesterol molecule during the production simulations in the 25 mol % cholesterol membrane.

cholesterol molecules, making it easier for the large hypericin molecules to incorporate. In the 25 mol % cholesterol membrane, this behavior was harder to determine with certainty due to the overall higher cholesterol concentration.

The minimum distance between any pair of atoms from either of the two hypericin molecules in each simulation and any of the cholesterol molecules was investigated during the production simulations (Figures 4 and 5) to explore if the hypericin molecules were able to interact with the cholesterol molecules. In the membrane with 9 mol % cholesterol, the minimum distance between Hy and cholesterol was in the range 0.25−1.25 nm, with an average distance of 0.56 nm. The distance between Hy-Br and Hy-4Br and cholesterol fluctuated more frequently than for Hy, varying between 0.2 and 1.3 nm for Hy-Br and between 0.2 and 1.1 nm for Hy-4Br, with an average distance of 0.63 nm for both molecules. In the 25 mol % cholesterol membrane, the distance between the hypericin molecules and cholesterol displayed less variation, with distances in the range of 0.2−1.0 nm and an average for Hy of 0.46 nm; for Hy-Br, 0.64 nm; and for Hy-4Br, 0.73 nm. All average distances are summarized in Table 1. The Hy molecules are obviously the ones located closest to cholesterol in both membranes, and in the 25 mol % cholesterol membrane, the minimum distance between Hy and cholesterol is shorter than in the 9 mol % cholesterol membrane. For Hy-Br, there is no significant difference between the two membranes, whereas for Hy-4Br the minimum distance is longer in the 25 mol % cholesterol membrane, nearly 3 Å longer than for Hy in the same membrane. We emphasize, however, that the trends observed should be taken with some caution given the limited amount of data.

Density profiles for the different systems are displayed in Figure 6 and show that the probability to find the hypericin

Table 1. Average Distances (in nm) between Any Pair of Atoms of a Hypericin Molecule and a Cholesterol Molecule Inside the Two Membranes during the Production Runs

molecule	9 mol % cholesterol	25 mol % cholesterol
Hy	0.56	0.46
Hy-Br	0.63	0.64
Hy-4Br	0.63	0.73

molecules close to the polar headgroups and the interface between the lipids and water is high. This being the densest region of the bilayer, it would not be favorable for the large and inflexible hypericin molecules to accumulate if it was not for the possibility to interact with water while still being embedded in the lipids. This is discussed further in connection with the radial distribution functions below. Comparing the two membranes reveals that Hy is found overall slightly closer to the lipid/water interface in the 9 mol % cholesterol membrane. For Hy-Br, the molecule that enters the lipids from water (right peak) ends up closer to the lipid/water interface than the molecule that was initially positioned in the middle of the bilayer. This is seen in both membranes. Hy-4Br displays wider density profiles than Hy and Hy-Br, in both membranes, and moves closer to the bilayer center than any of the others. This results in less interaction with water and is supported by observations made in a pure DPPC membrane.[39] Concluded from the density profiles is that at least one of the two Hy and Hy-Br molecules in each simulation is located closer to the lipid/water interface in the 9 mol % cholesterol membrane. Similar density profiles have been found for smaller drug molecules such as psoralens and 5-aminolevulinic acid and derivatives thereof; however, these molecules were located slightly closer to the bilayer center.[88,89]

In natural membranes, unsaturated lipids are important constituents, especially in the formation of raft domains. Due to the use of saturated lipids in the present study, possible interactions between the hypericin molecules and unsaturated lipids, as well as between cholesterol and unsaturated lipids was not accounted for, which could affect the partition and behavior of the molecules. It has been found that cholesterol interacts stronger with saturated lipids than unsaturated ones, resulting in more pronounced effects on the structure of the membrane, including condensing and ordering aspects.[27] Consequently, this affects the behavior of small molecules, such as hypericin, in the membranes. As an initial study of the behavior of hypericin derivatives in cholesterol containing membranes, and to enable comparisons with earlier work on hypericin in purely saturated bilayers, we used saturated lipids also in the present study. As a next step, in order to follow up this study, unsaturated lipids would be included for comparison.

In cholesterol-containing membranes, the lipids are more ordered and their tails more aligned to the bilayer normal, compared to in a pure DPPC membrane. This results in a larger bilayer thickness and is seen by comparing the DPPC density profile for the 25 mol % cholesterol membrane in Figure 6 with the DPPC density profiles for the pure lipid membrane.[39] The bilayer thickness is increased by a few Ångstroms in the cholesterol-containing membrane. In the 9 mol % cholesterol membrane, the bilayer thickness is approximately the same as in the pure DPPC membrane. However, the fact that the bilayer thickness is increased does not necessarily mean that each monolayer thickness is increased in the 25 mol % cholesterol membrane but is rather a result of the monolayers being more separated, resulting in a decrease in density in the center of the bilayer (Figure 6). These findings are in agreement with previous observations that the hydrophobic thickness is increased and the electron density in the center of the bilayer is decreased in cholesterol-containing membranes.[17,24] In the 9 mol % cholesterol membrane, the monolayer separation is similar to the one in the pure DPPC membrane, indicated by the higher density in the bilayer center. The increased free space in the middle of the 25 mol % cholesterol membrane could be expected to result in a reduced probability of locating the hydrophobic hypericin molecules in that region, even more than in the more compact membranes. This is supported by the calculated free energy profiles for the transport process through the membrane and is further discussed below.

A test set of simulations with 10 hypericin (Hy) molecules initially placed in the water region of the two systems provided information about interactions between the molecules (data not shown). It was clear that in the water phase the molecules tend to stack together due to the nonfavorable polar environment. Previous studies have confirmed that hypericin molecules interact with each other in solution, forming dimers when the concentration is low[90] and H aggregates of at least four molecules positioned face to face when the concentration is higher.[91] It is clear from the simulations performed herein that the hypericin molecules interact strongly with each other in conformations of either two or four molecules in the water phase; however, whether dimers or H aggregates are predominantly formed is difficult to determine due to the high degree of movement in the system. The aggregation did not seem to affect the ability to enter the lipids, and the molecules remained stacked together also within the lipids, indicating that these interactions are favorable also in a nonpolar environment. It has previously been observed that the photodynamic properties of hypericin are altered by aggregation, resulting in a decreased singlet oxygen yield,[90] an issue that needs to be considered if the hypericin molecules are to be activated by light within a membrane.

Radial distribution functions between oxygen atoms on the hypericin derivatives and hydrogen atoms in the surrounding water (Figure 7A) and between polar hydrogen atoms on the hypericin derivatives and oxygen atoms in the surrounding water (Figure 7B) were calculated for both membranes. The first peak in both figures (at ~0.18 nm) corresponds to a hydrogen bond. The following peak in Figure 7A corresponds to a second hydrogen in the same water molecule or a second solvation shell, whereas the second peak in Figure 7B corresponds to a second solvation shell of water. Following this, there is an increase in amplitude of the radial distribution functions as more and more water molecules are included in shells of higher order.

The peaks corresponding to hydrogen bonds suggest that the hypericin molecules, to a greater or smaller extent, interact with water as they accumulate in the region close to the interface between the lipids and water. In a pure DPPC membrane, a clear trend was observed for the radial distribution functions, with Hy displaying the highest radial distribution functions overall, followed by Hy-Br and Hy-4Br, respectively.[39] Such a clear trend cannot be observed in the cholesterol-containing membranes. In the 9 mol % cholesterol membrane, Hy-Br displays the highest radial distribution function for a hydrogen bond between oxygen atoms on hypericin and hydrogen atoms in water followed by Hy and Hy-4Br, respectively. This feature can be explained by the finding that one of the Hy-Br molecules was located very close to the lipid water interface, as seen in the density profiles. However,

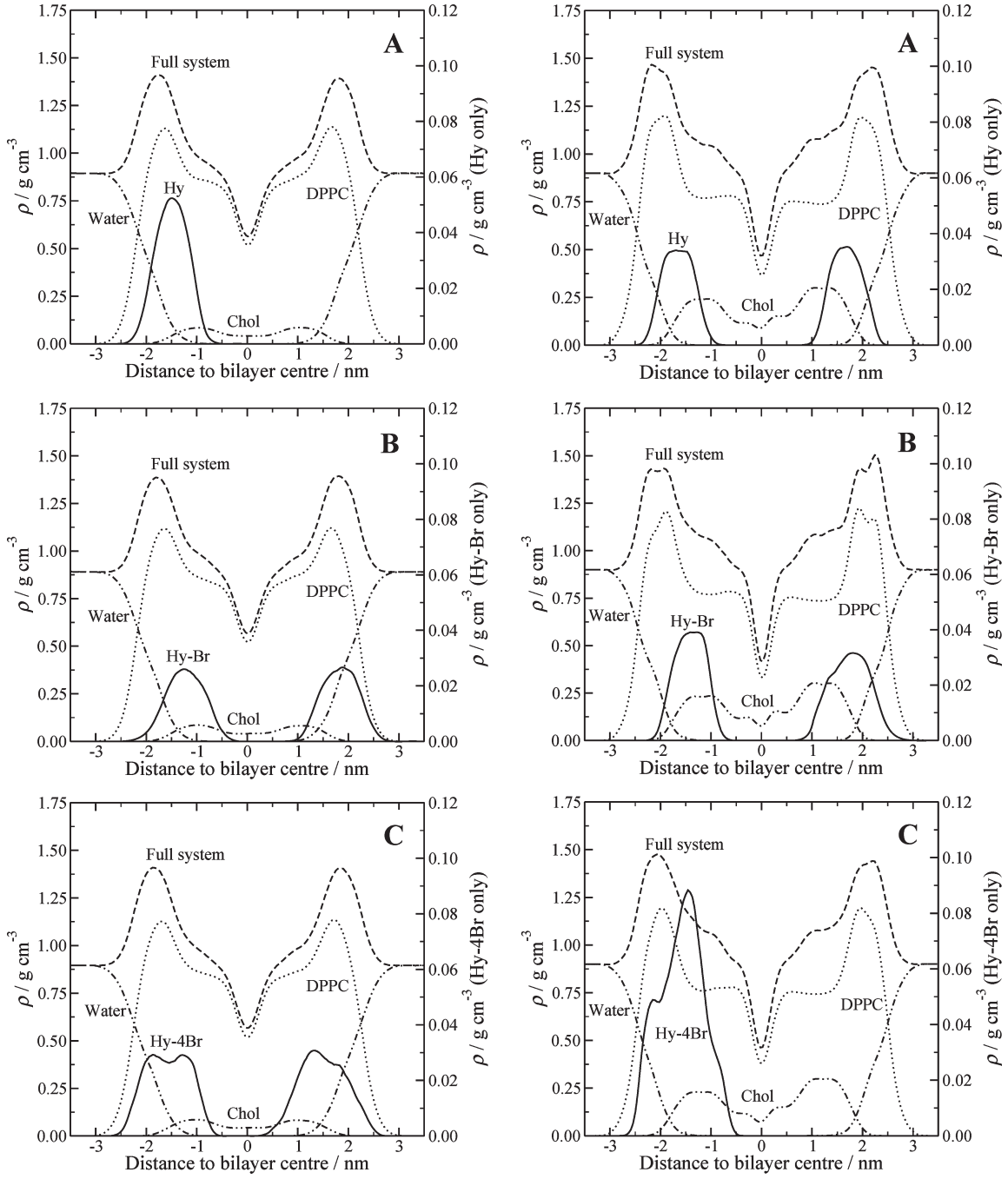

Figure 6. Density profiles for two hypericin derivatives (A, Hy; B, Hy-Br; C, Hy-4Br) in the DPPC bilayer with 9% cholesterol (left) and 25% cholesterol (right).

Hy displays the highest radial distribution function for a hydrogen bond between hydrogen atoms of hypericin and oxygen atoms in water, albeit very low, followed by even lower amplitudes for Hy-Br and Hy-4Br. In the 25 mol % cholesterol membrane, Hy displays the highest radial distribution function for a hydrogen bond between oxygen atoms on hypericin and hydrogen atoms in water followed by Hy-Br and Hy-4Br at equal amplitudes, whereas Hy and Hy-Br display the highest radial distribution functions for hydrogen bonds between hydrogen atoms of hypericin and oxygen atoms in water. Common for all membranes, with and without cholesterol, is that Hy-4Br overall displays the lowest radial distribution functions. This is explained by the fact that this molecule was moving closer to the bilayer middle during the simulations in both membranes, hence reducing the ability to interact with water.

The mean-square displacement (MSD)[92] reveals details about the movements of a molecule inside the bilayer and is defined by

$$\mathrm{MSD}(t) = \langle |\vec{r}(t) - \vec{r}(0)|^2 \rangle \qquad (7)$$

where $\vec{r}(0)$ and $\vec{r}(t)$ are the positions of a particle at time $t = 0$ and at a certain time t.

The brackets indicate a time average over all similar particles and over different time origins along the simulation. The Einstein

dx.doi.org/10.1021/ct100528u |J. Chem. Theory Comput. 2011, 7, 560–574

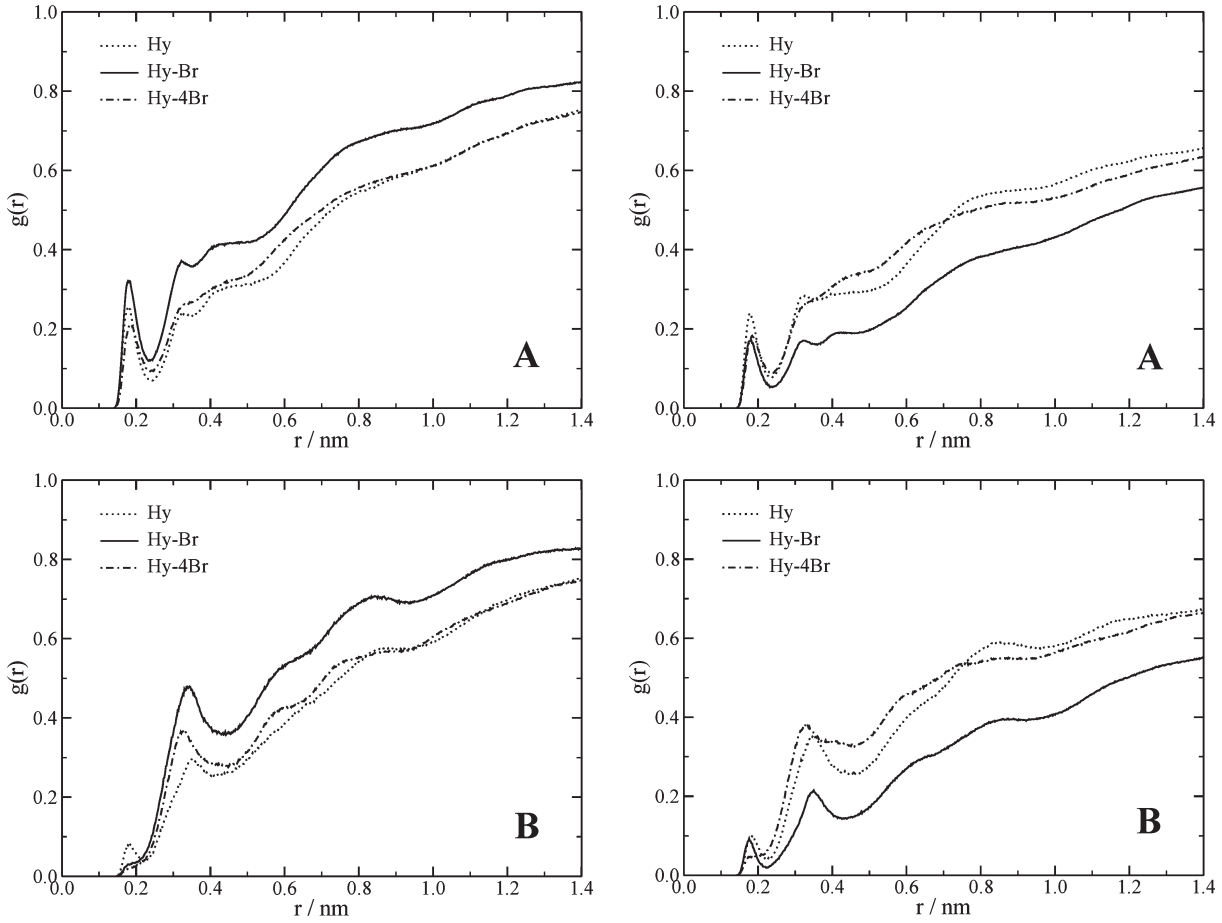

Figure 7. Radial distribution functions between (A) oxygen atoms on the hypericin derivatives and hydrogen atoms in the surrounding water and (B) polar hydrogen atoms on the hypericin derivatives and oxygen atoms in the surrounding water in the 9 mol % (left) and 25 mol % cholesterol membranes (right).

relation allows for the calculation of the diffusion coefficient, D, at sufficiently long simulation times:[92]

$$D = \lim_{t\to\infty} \frac{1}{2dt}\langle |r_i(t) - r_i(0)|^2 \rangle \qquad (8)$$

where d is the dimensionality of the space.

This way, one can obtain the MSD for the molecules moving in the bilayer plane ($d = 2$) and along the bilayer normal ($d = 1$), respectively. The MSD provides a measure of the average distance a molecule travels in the system, and the growth rate of the MSD depends on how often the molecule collides, i.e., a measure of the ease of diffusion of the molecule.

Like other molecules diffusing in confined media, the hypericin molecules never reach the Einsteinian limit of proper diffusion within the limited time of the simulation, and anomalous diffusion occurs where MSD is proportional to t^n, with $0 < n < 1$. The implication is that a direct comparison with experimental diffusion coefficients cannot be made. However, on the basis of the MSD, one can state which molecules have a higher or lower diffusive regime. The MSDs of the hypericin derivatives in the bilayer plane and along the normal of the bilayer (z direction) in the two membranes are displayed in Figure 8A and B, respectively. The addition of a bromine atom to the hypericin molecule does not significantly affect the movement in the bilayer plane in the 9 mol % cholesterol membrane, whereas the addition of four bromine atoms makes the molecule move more easily. Despite the fact that Hy-4Br is heavier than the two other molecules, its movement in the bilayer plane is faster due to a lower propensity of forming hydrogen bonds with water, as seen above. In the 25 mol % cholesterol membrane, however, the movement in the bilayer plane is highest for Hy, followed by Hy-4Br and Hy-Br, and the movement of both Hy and Hy-4Br is considerably higher here than in the membrane of lower cholesterol concentration. This situation does not reflect the hydrogen bond capability with water, as it was shown above that Hy exhibits the highest radial distribution functions in the 25 mol % cholesterol membrane. The movement of all molecules in the bilayer plane of the 9 mol % cholesterol membrane is slower than in a pure DPPC membrane.[39] The movement of Hy in the bilayer plane of the 25 mol % cholesterol membrane is similar to that in a pure DPPC membrane, whereas for Hy-Br and Hy-4Br the movement is slower.

The MSDs for the molecules along the bilayer normal of the two membranes are displayed in Figure 8B. This movement is, as opposed to the movement in the bilayer plane, finite and should hence be interpreted with caution. The MSD profiles in the direction of the bilayer normal of the 9 mol % cholesterol membrane are similar, and on the same order of magnitude, as the ones obtained in a pure DPPC membrane, displaying the slowest movement for Hy and similar, yet faster, movement for Hy-Br and Hy-4Br,[39] and overall slightly faster than in the 25 mol % cholesterol membrane. It is clearly seen that the

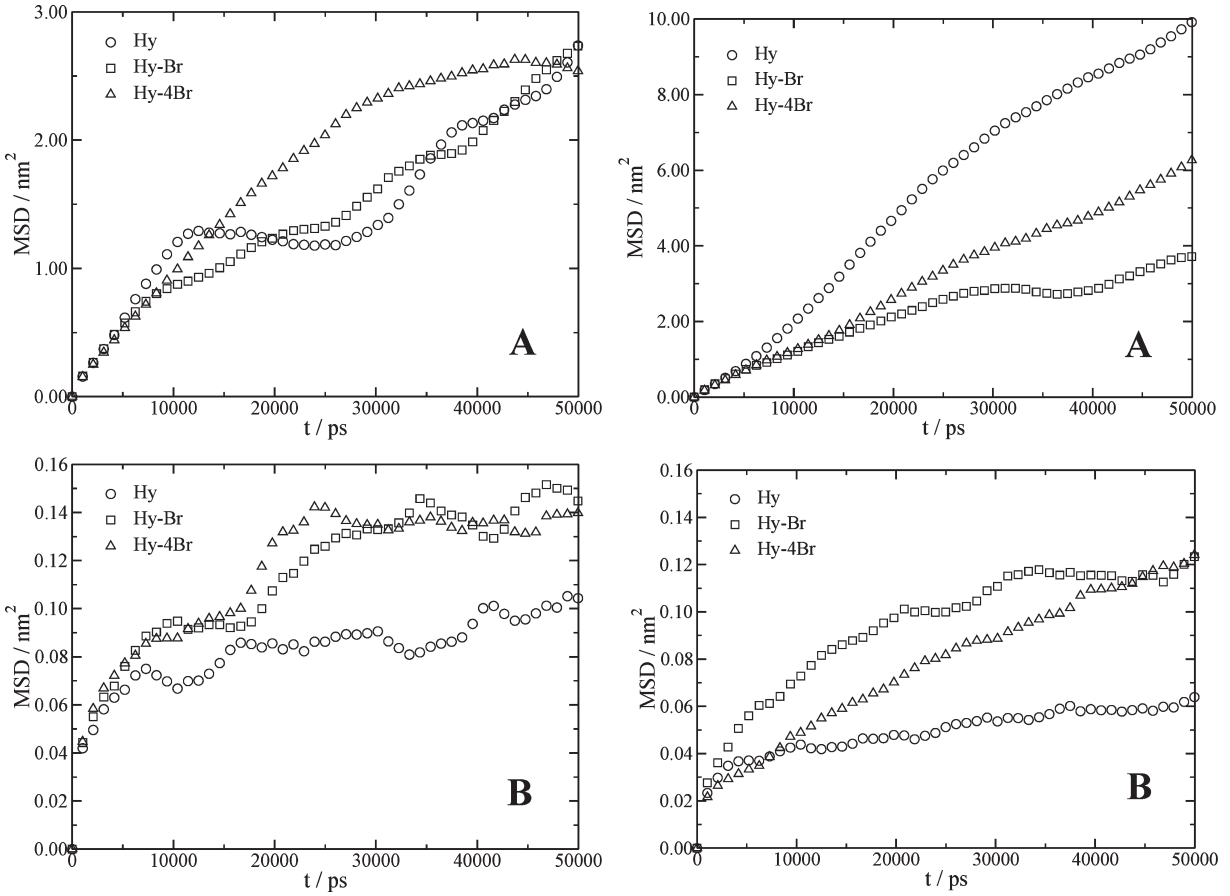

Figure 8. MSD in (A) the *xy* plane and (B) the direction normal to the bilayer in the 9 mol % (left) and 25 mol % cholesterol membrane (right). Note the different scales on the *y* axes in A.

movement in the bilayer plane is significantly higher than in the direction of the bilayer normal.

The local diffusion coefficients are displayed in Figure 9 as functions of the distance to the bilayer center and were obtained by integrating the fitted autocorrelation functions (eq 4). It is clear that the diffusion of the molecules is low inside the lipids, whereas in the water, the diffusion is faster, which is seen by the increase in diffusion in the far left and far right regions of the graphs in Figure 9. As we only studied the hypericin molecules at a distance of at most 3.3 nm from the bilayer center, the molecules are at this distance still interacting with the lipids, which allow for less free movement of the molecules compared to bulk water. In the pure DPPC system, in which systems at larger distances from the bilayer center (the diffusion further out in the water phase) were studied, diffusion in the water phase was at least 10 times faster than inside the lipids, and strongly dependent on the size of the molecules.[39] We expect diffusion coefficients on the same order of magnitude far out in the water phase of the cholesterol-containing systems as well.

In the 9 mol % cholesterol membrane, the diffusion of all three molecules inside the lipids was relatively constant, with a small decrease in diffusion for Hy and Hy-4Br and a small increase in diffusion for Hy-Br, in the very middle of the membrane. Hy shows the lowest diffusion at the bilayer center. However, in the 25 mol % cholesterol membrane, the diffusion close to the middle of the membrane is significantly increased compared to further out in the lipids and also compared to the middle of the 9 mol % cholesterol membrane. The large increase in diffusion is due to the increased free space in the middle of the high cholesterol membrane, in which the monolayers are more separated. This free space allows for fast diffusion due to few interactions with lipid molecules. Hy displays the fastest diffusion in the middle, followed by Hy-Br and Hy-4Br. In the remaining lipid region, the diffusion is overall lower than in the membrane containing a lower amount of cholesterol.

Free energy profiles for the transport process from water and into the lipids, as a function of the distance to the bilayer center, were calculated using the potential of mean force formalism outlined above[93] and are displayed in Figure 10 together with the data obtained in the pure DPPC membrane. In a previous study performed using the same technique, but with only 2 ns production runs (we used 4 ns in water and 10 ns in the lipid bilayer), errors in free energy were found to be in the range of 0.7−4 kJ/mol in the bilayer middle, the region with the largest errors.[94] As the simulations performed in the present study were longer than the ones for which these errors were calculated, we expect the errors herein to be in the same range, if not smaller.

For the hypericin molecules, local minima were found in the region 1−2 nm from the bilayer center, close to the polar headgroup region where the molecules were found to accumulate during the unconstrained simulations. As the molecules continue moving across the bilayer, the free energy increases and shows a maximum in the very middle of the bilayer. In both cholesterol-containing membranes, Hy-Br shows the deepest minimum close to the polar headgroups, followed by Hy-4Br and Hy. For Hy-Br, the minimum is deeper in the 25 mol % cholesterol membrane,

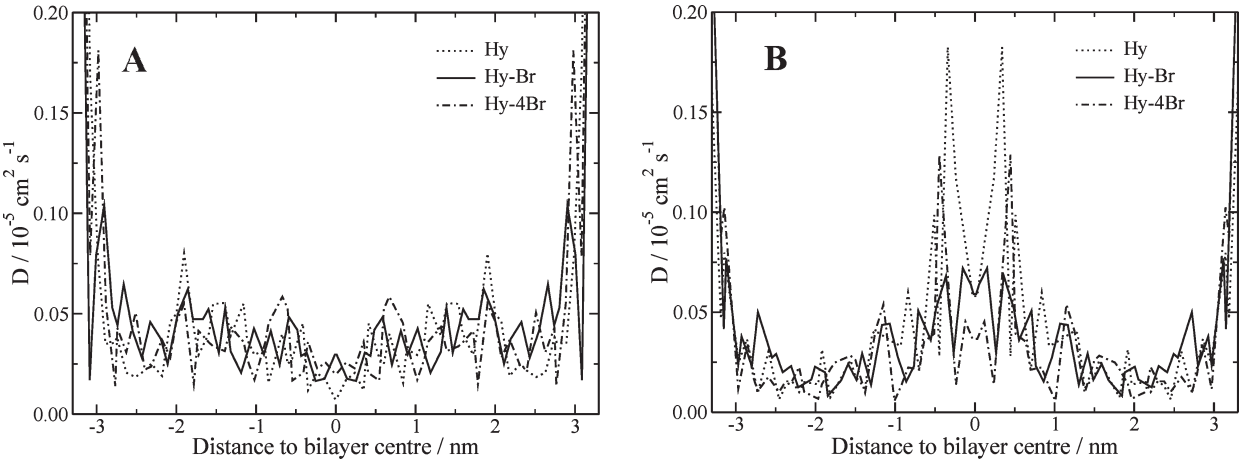

Figure 9. Local diffusion coefficients of the hypericin derivatives in (A) 9 mol % and (B) 25 mol % cholesterol membranes, as a function of the distance to the bilayer middle.

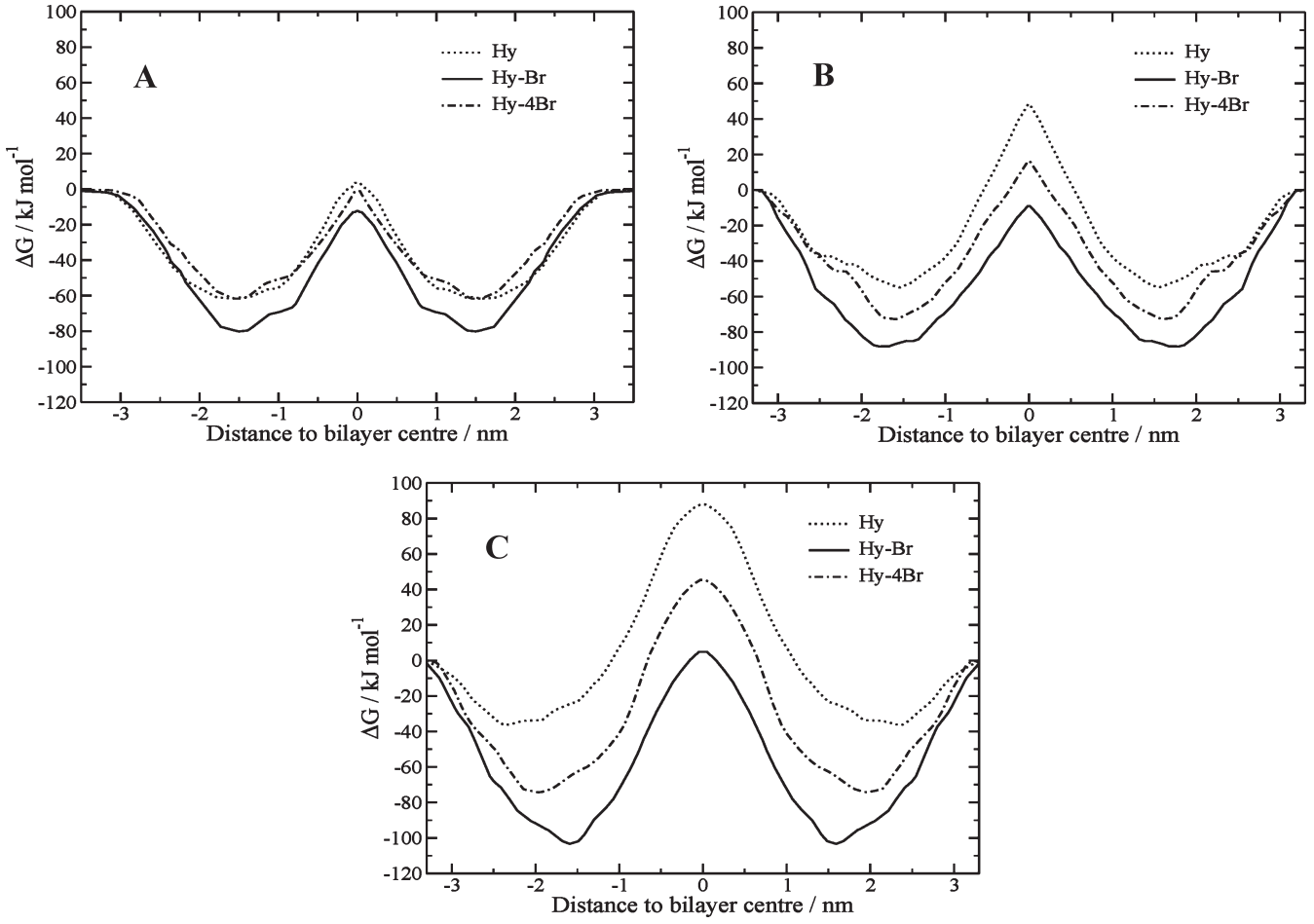

Figure 10. Free energy profiles for the hypericin derivatives inside the (A) 0 mol %, (B) 9 mol %, and (C) 25 mol % cholesterol membranes.

whereas for Hy-4Br, the minimum is more or less at the same depth in the two membranes, and for Hy, the minimum is less deep in the 25 mol % cholesterol membrane. In the middle of the bilayer, the free energy of the molecules follows the same order, with Hy-Br displaying the lowest energy. All three molecules display higher energy barriers in the high cholesterol membrane, with positive ΔG values compared to when in water. In the 9 mol % cholesterol membrane, however, Hy-Br displays a negative overall free energy also in the bilayer center.

In the low cholesterol-containing membrane, the local minima of the molecules are found further out from the bilayer center with a larger decrease in free energy; accordingly the minimum of Hy-Br is found further toward the lipid/water interface, followed by Hy-4Br and Hy. Interestingly, in the high cholesterol

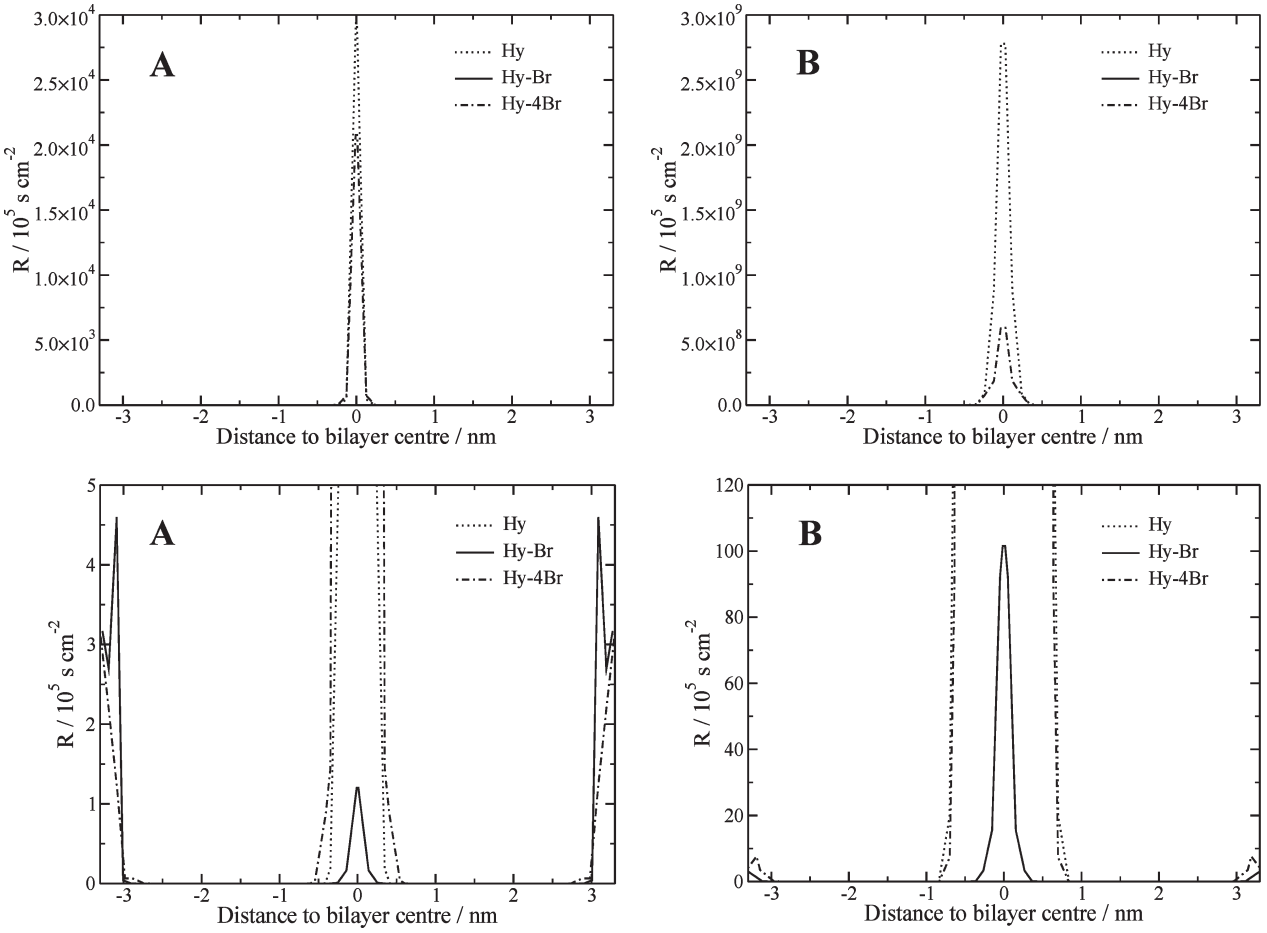

Figure 11. Local resistance profiles of the hypericin derivatives in (A) 9 mol % and (B) 25 mol % cholesterol membranes, as a function of the distance to the bilayer middle. The Hy profile was scaled down by a factor 3×10^5 in the 9 mol % cholesterol membrane and by a factor 10^6 in the 25 mol % cholesterol membrane. Magnification of the local resistance profiles of Hy-Br are displayed in the lower graphs. Note the different scales on the *y* axis of the graphs.

membrane, the opposite situation is observed. Here, the minimum lies closer to the bilayer center with a larger decrease in free energy, generating the minimum of Hy-Br significantly closer to the bilayer center than the two other molecules.

The free energy maxima of the molecules in the 25 mol % cholesterol membrane are clearly more rounded than the narrow maxima found with a lower cholesterol concentration. This is due to the fact that, as discussed above, the two monolayers are more separated in the membrane with higher cholesterol content. The free space in the middle of the membrane is also responsible for the larger increase in free energy in this region compared to in the membrane with a lower cholesterol content. The free space constitutes a less hydrophobic region offering less possible interactions with lipids, in which it is not favorable for the hydrophobic molecules to be located, and thereby generating a large increase in free energy for transport process into/across that region.

In the pure DPPC bilayer, Hy-Br was also found to display the lowest overall change in free energy along the bilayer normal (Figure 10A).[39] In the 9 mol % cholesterol membrane, Hy-Br and Hy-4Br show deeper free energy minima in the headgroup region compared to the pure DPPC membrane, whereas Hy displays an increase. In the middle of the bilayer, the free energy is increased (more positive) for all three molecules. Only Hy-Br still displays a negative free energy, however slightly less negative than without cholesterol present. Hy-4Br, which displayed a small negative change in free energy in the middle of the pure DPPC membrane, is now on the positive side. In the 25 mol % cholesterol membrane, the same pattern is seen when comparing with the pure DPPC membrane, although with larger overall changes than in the 9 mol % cholesterol membrane. It is clear that Hy is most negatively affected by the inclusion of cholesterol in the membrane, displaying a significant increase in free energy both in the middle of the bilayer and close to the polar headgroups.

The local resistance was calculated from the local diffusion coefficients and the free energy profiles using eq 6, and the resulting profiles are displayed in Figure 11. An increase in resistance is seen for all molecules in the middle of the bilayer; however, the magnitude of this peak clearly differs for the three molecules. The resistance for Hy is significantly higher than for the two other molecules in both membranes, and therefore it was scaled down to more clearly display the profiles. The resistance for Hy-Br is considerably lower than for the two other molecules in both membranes, and its profiles can only be seen in the lower graphs of Figure 11 where we show a magnification of the low resistance region. In the 25 mol % cholesterol membrane, the resistances for the molecules are overall higher compared to when the cholesterol concentration is lower. In both membranes, the Hy and Hy-4Br resistances in the middle are considerably

Table 2. Permeability Coefficients (in cm/s) of the Hypericin Derivatives inside the Membranes without and with Cholesterol

molecule	0 mol % cholesterol[39]	9 mol % cholesterol	25 mol % cholesterol
Hy	4.21×10^{-4}	8.25×10^{-12}	1.63×10^{-17}
Hy-Br	4.94×10^{-3}	5.49×10^{-3}	4.12×10^{-4}
Hy-4Br	1.51×10^{-3}	3.31×10^{-6}	6.93×10^{-11}

higher than in the water phase, as is seen in the lower graphs of Figure 11. For Hy-Br, however, the resistance in the middle is higher than in water in the 25 mol % cholesterol membrane, whereas in the 9 mol % cholesterol membrane, the resistance in the middle is lower than that in water. The free energy is the major contributor to the shape of the resistance profiles, with an increase in free energy giving an increase in resistance. The lowest free energy of Hy-Br in the middle of the membrane therefore generates the lowest resistance, and the opposite for Hy. The molecules exhibit higher resistances in the middle of the cholesterol-containing membranes than in a pure DPPC membrane.[39]

Permeability coefficients were calculated by integrating the resistance profiles across the bilayer and are displayed in Table 2. In both cholesterol-containing membranes, the permeation decreases in the order Hy-Br > Hy-4Br > Hy, in agreement with the findings in a pure DPPC membrane,[39] for which data are also included in Table 2. In the 25 mol % cholesterol membrane, the permeation is overall slower than when the cholesterol concentration is lower. The difference in permeation of Hy-Br in the two cholesterol-containing membranes is only 1 order of magnitude, whereas for the two other molecules, the difference is significantly larger. The permeation of Hy-Br is not considerably affected by the inclusion of cholesterol, when compared to that in a pure DPPC membrane.[39] In fact, the permeation in the low cholesterol membrane is slightly faster than in the pure DPPC membrane. For the two other molecules, the permeation is considerably reduced compared to the pure DPPC membrane. As mentioned above, the resistance, and thereby the permeability, strongly depends on the free energy, and with an increase in energy follows a decrease in permeation. This supports the finding of Hy-Br displaying the fastest permeation (large permeability coefficient) as it exhibits the lowest free energy, both close to the polar headgroups and in the center of the bilayer. Hy-Br was also displaying the largest movement in the z direction of the bilayer, as seen above. These results suggest that Hy-Br most likely would have the highest probability of penetrating the plasma membrane and reach the interior of the cell, whereas the two other molecules would be more prone to residing in the membrane and from there cause photodamage.

Experimentally, it has been shown that halogenated drugs display larger permeability coefficients through lipid membranes;[63] however, the permeability of the molecules can also be reduced by the addition of large and heavy substituents. This can explain the reduced permeability of tetra-brominated hypericin compared with the monobrominated one.

The finding that Hy displays the slowest diffusion in the membranes can be explained by the fact that this molecule was found to reside closer to cholesterol molecules in both membranes, and it also forms hydrogen bonds to the water phase. Even though the distance between Hy and cholesterol was never short enough to allow direct interactions, the ordering of the lipids close to cholesterol molecules can affect the permeability of the hypericin molecule.

4. CONCLUSIONS

The behavior of hypericin, a natural compound possessing photodynamic properties, and its mono- and tetra-brominated derivatives was studied in DPPC lipid membranes containing 9 and 25 mol % cholesterol, respectively, by means of molecular dynamics simulations. The three molecules were found to accumulate in the region close to the polar headgroups of the lipids, close to the interface between the lipids and water. This location enables interactions between the hydroxyl groups of the hypericin molecules and water, supported by hydrogen bonds found in the radial distribution functions. Overall, the hypericin molecules in the 25 mol % cholesterol membrane were found slightly closer to the bilayer middle than in the low cholesterol membrane. With a high amount of cholesterol present in the membrane, the two monlayers are slightly separated and allow for fast diffusion in that region. However, this region also offers fewer lipid interactions with the hydrophobic hypericin molecules, making it a nonfavorable location to reside in, indicated by the large increase in free energy for the transport process of the molecules into that region. Close to the polar headgroups, where the hypericin molecules were found to accumulate, the free energy profiles showed local minima. The size of these minima was dependent on the molecule and the amount of cholesterol in the membrane. The permeability coefficients were overall lower in the high cholesterol membrane. Hy-Br displayed the largest decrease in free energy both in the middle of the bilayer and close to the headgroups, as well as the highest permeability coefficients in both membranes. This indicates that this molecule would have the highest probably to penetrate a plasma membrane, independently of the cholesterol concentration, and reach the interior of a cell. The two other molecules, in particular Hy, exhibit significantly lower permeability and are expected to be found within the membrane.

■ ASSOCIATED CONTENT

Supporting Information. Cholesterol topology, hypericin topology, Hy-Br topology, Hy-4Br topology, evolution of the area per lipid during the last 10 ns of the equilibration of the cholesterol containing membranes, and RDFs for DPPC-Chol and Chol-Chol center-of-mass during production runs (100 ns) for each membrane and each hypericin system. This material is available free of charge via the Internet at http://pubs.acs.org.

■ AUTHOR INFORMATION

Corresponding Author

*E-mail: leif.eriksson@nuigalway.ie.

■ ACKNOWLEDGMENT

The National University of Ireland—Galway is gratefully acknowledged for financial support. We also acknowledge Dr. Daniel dos Santos (Univ. of Lisbon) for valuable discussions.

■ REFERENCES

(1) De Kruyff, B.; De Greef, W. J.; Van Eyk, R. V. W.; Demel, R. A.; Van Deene, L. *Biochim. Biophys. Acta* **1973**, *298*, 479–499.

(2) Lange, Y.; Swaisgood, M. H.; Ramos, B. V.; Steck, T. L. *J. Biol. Chem.* **1989**, *264*, 3786–3793.

(3) Bretscher, M. S.; Munro, S. *Science* **1993**, *261*, 1280–1281.
(4) Sackmann, E. In *Structure and dynamics of membranes*; Lipowsky, R., Sackmann, E., Eds.; Elsevier: Amsterdam, 1995; pp 1−62.
(5) Ipsen, J. H.; Karlström, G.; Mouritsen, O. G.; Wennerström, H.; Zuckermann, M. J. *Biochim. Biophys. Acta* **1987**, *905*, 162–172.
(6) Vist, M. R.; Davis, J. H. *Biochemistry* **1990**, *29*, 451–464.
(7) Boggs, J. M.; Hsia, J. C. *Biochim. Biophys. Acta* **1972**, *290*, 32–42.
(8) Oldfield, E.; Meadows, M.; Rice, D.; Jacobs, R. *Biochemistry* **1978**, *17*, 2727–2740.
(9) Marsh, D.; Smith, I. C. P. *Biochim. Biophys. Acta* **1973**, *298*, 133–144.
(10) Yeagle, P. L. *Biochim. Biophys. Acta* **1985**, *822*, 267–287.
(11) Simons, K.; Toomre, D. *Nat. Rev. Mol. Cell Biol.* **2000**, *1*, 31–39.
(12) Scott, H. L.; Kalaskar, S. *Biochemistry* **1989**, *28*, 3687–3691.
(13) Scott, H. L. *Biophys. J.* **1991**, *59*, 445–455.
(14) Edholm, O.; Nyberg, A. M. *Biophys. J.* **1992**, *63*, 1081–1089.
(15) Hofsäss, C.; Lindahl, E.; Edholm, O. *Biophys. J.* **2003**, *84*, 2192–2206.
(16) Niemelä, P. S.; Ollila, S.; Hyvönen, M. T.; Karttunen, M.; Vattulainen, I. *PLos Comput. Biol.* **2007**, *3*, 304–312.
(17) Smondyrev, A. M.; Berkowitz, M. L. *Biophys. J.* **1999**, *77*, 2075–2089.
(18) Pasenkiewicz-Gierula, M.; Róg, T.; Kitamura, K.; Kusumi, A. *Biophys. J.* **2000**, *78*, 1376–1389.
(19) Chiu, S. W.; Jakobsson, E.; Scott, H. L. *J. Chem. Phys.* **2001**, *114*, 5435–5443.
(20) Róg, T.; Pasenkiewicz-Gierula, M. *Biophys. J.* **2001**, *81*, 2190–2202.
(21) Chiu, S. W.; Jakobsson, E.; Mashl, R. J.; Scott, H. L. *Biophys. J.* **2002**, *83*, 1842–1853.
(22) Falck, E.; Patra, M.; Karttunen, M.; Hyvönen, M. T.; Vattulainen, I. *Biophys. J.* **2004**, *87*, 1076–1091.
(23) Tu, K. C.; Klein, M. L.; Tobias, D. J. *Biophys. J.* **1998**, *75*, 2147–2156.
(24) Douliez, J. P.; Leonard, A.; Dufourc, E. J. *J. Phys. Chem.* **1996**, *100*, 18450–18457.
(25) Martinez-Seara, H.; Róg, T.; Karttunen, M.; Vattulainen, I.; Reigada, R. *PLos One* paper: e11162, pages 1−11.
(26) Róg, T.; Pasenkiewicz-Gierula, M.; Vattulainen, I.; Karttunen, M. *Biophys. J.* **2007**, *92*, 3346–3357.
(27) Róg, T.; Pasenkiewicz-Gierula, M. *Biochimie* **2006**, *88*, 449–460.
(28) Pitman, M. C.; Suits, F.; MacKerell, A. D.; Feller, S. E. *Biochemistry* **2004**, *43*, 15318–15328.
(29) Martinez-Seara, H.; Róg, T.; Pasenkiewicz-Gierula, M.; Vattulainen, I.; Karttunen, M.; Reigada, R. *J. Phys. Chem. B* **2007**, *111*, 11162–11168.
(30) Martinez-Seara, H.; Róg, T.; Pasenkiewicz-Gierula, M.; Vattulainen, I.; Karttunen, M.; Reigada, R. *Biophys. J.* **2008**, *95*, 3295–3305.
(31) Papahadjopoulos, D.; Nir, S.; Ohki, S. *Biochim. Biophys. Acta* **1972**, *266*, 561–583.
(32) Finkelstein, A.; Cass, A. *Nature* **1967**, *216*, 717–718.
(33) Zhao, L. Y.; Feng, S. S. *J. Colloid Interface Sci.* **2006**, *300*, 314–326.
(34) Gere-Paszti, E.; Farkas, O.; Prodan, M.; Forgacs, E. *Chromatographia* **2003**, *57*, 599–604.
(35) Söderlund, T.; Lehtonen, J. Y. A.; Kinnunen, P. K. J. *Mol. Pharmacol.* **1999**, *55*, 32–38.
(36) Ghannam, M. M.; Mady, M. M.; Khalil, W. A. *Biophys. Chem.* **1999**, *80*, 31–40.
(37) Prenner, E. J.; Lewis, R.; Jelokhani-Niaraki, M.; Hodges, R. S.; McElhaney, R. N. *Biochim. Biophys. Acta Biomembr.* **2001**, *1510*, 83–92.
(38) Ji, S. R.; Wu, Y.; Sui, S. F. *J. Biol. Chem.* **2002**, *277*, 6273–6279.
(39) Eriksson, E. S. E.; dos Santos, D. J. V. A.; Guedes, R. C.; Eriksson, L. A. *J. Chem. Theory Comput.* **2009**, *5*, 3139–3149.
(40) Linde, K.; Mulrow, C. D.; Berner, M.; Egger, M. *Cochrane Database Syst. Rev.* **2005**, 73.
(41) Meruelo, D.; Lavie, G.; Lavie, D. *Proc. Natl. Acad. Sci. U.S.A.* **1988**, *85*, 5230–5234.
(42) Lopezbazzocchi, I.; Hudson, J. B.; Towers, G. H. N. *Photochem. Photobiol.* **1991**, *54*, 95–98.
(43) Hudson, J. B.; Lopezbazzocchi, I.; Towers, G. H. N. *Antivir. Res.* **1991**, *15*, 101–112.
(44) Degar, S.; Prince, A. M.; Pascual, D.; Lavie, G.; Levin, B.; Mazur, Y.; Lavie, D.; Ehrlich, L. S.; Carter, C.; Meruelo, D. *AIDS Res. Hum. Retrovir.* **1992**, *8*, 1929–1936.
(45) Moraleda, G.; Wu, T. T.; Jilbert, A. R.; Aldrich, C. E.; Condreay, L. D.; Larsen, S. H.; Tang, J. C.; Colacino, J. M.; Mason, W. S. *Antiviral Res.* **1993**, *20*, 235–247.
(46) Lenard, J.; Rabson, A.; Vanderoef, R. *Proc. Natl. Acad. Sci. U.S.A.* **1993**, *90*, 158–162.
(47) Thomas, C.; Pardini, R. S. *Photochem. Photobiol.* **1992**, *55*, 831–837.
(48) Andreoni, A.; Colasanti, A.; Colasanti, P.; Mastrocinque, M.; Riccio, P.; Roberti, G. *Photochem. Photobiol.* **1994**, *59*, 529–533.
(49) VanderWerf, Q. M.; Saxton, R. E.; Chang, A.; Horton, D.; Paiva, M. B.; Anderson, J.; Foote, C.; Soudant, J.; Mathey, A.; Castro, D. J. *Laryngoscope* **1996**, *106*, 479–483.
(50) Liu, C. D.; Kwan, D.; Saxton, R. E.; McFadden, D. W. *J. Surg. Res.* **2000**, *93*, 137–143.
(51) D'Hallewin, M. A.; De Witte, P. A.; Waelkens, E.; Merlevede, W.; Baert, L. *J. Urol.* **2000**, *164*, 349–351.
(52) D'Hallewin, M. A.; Kamuhabwa, A. R.; Roskams, T.; De Witte, P. A. M.; Baert, L. *BJU Int.* **2002**, *89*, 760–763.
(53) Pytel, A.; Schmeller, N. *Urology* **2002**, *59*, 216–219.
(54) Delaey, E.; Zupko, I.; Chen, B.; Derycke, A.; Van Laar, F.; De Vos, D.; De Witte, P. *Int. J. Oncol.* **2003**, *23*, 519–524.
(55) Guedes, R. C.; Eriksson, L. A. *J. Photochem. Photobiol. Chem.* **2006**, *178*, 41–49.
(56) Hudson, J. B.; Delaey, E.; de Witte, P. A. *Photochem. Photobiol.* **1999**, *70*, 820–822.
(57) Senthil, V.; Jones, L. R.; Senthil, K.; Grossweiner, L. I. *Photochem. Photobiol.* **1994**, *59*, 40–47.
(58) Chaloupka, R.; Obsil, T.; Plasek, J.; Sureau, F. *Biochim. Biophys. Acta Biomembr.* **1999**, *1418*, 39–47.
(59) Ho, Y. F.; Wu, M. H.; Cheng, B. H.; Chen, Y. W.; Shih, M. C. *Biochim. Biophys. Acta Biomembr.* **2009**, *1788*, 1287–1295.
(60) Chen, B.; Xu, Y.; Roskams, T.; Delaey, E.; Agostinis, P.; Vandenheede, J. R.; de Witte, P. *Int. J. Canc.* **2001**, *93*, 275–282.
(61) Kascakova, S.; Refregiers, M.; Jancura, D.; Sureau, F.; Maurizot, J. C.; Miskovsky, P. *Photochem. Photobiol.* **2005**, *81*, 1395–1403.
(62) Mukheriee, P.; Adhikary, R.; Halder, M.; Petrich, J. W.; Miskovsky, P. *Photochem. Photobiol.* **2008**, *84*, 706–712.
(63) Gerebtzoff, G.; Li-Blatter, X.; Fischer, H.; Frentzel, A.; Seelig, A. *ChemBioChem* **2004**, *5*, 676–684.
(64) Hess, B.; Kutzner, C.; van der Spoel, D.; Lindahl, E. *J. Chem. Theor. Comput.* **2008**, *4*, 435–447.
(65) Tieleman, D. P.; Berendsen, H. J. C. *J. Chem. Phys.* **1996**, *105*, 4871−4880.
(66) Patra, M.; Karttunen, M.; Hyvönen, M. T.; Falck, E.; Lindqvist, P.; Vattulainen, I. *Biophys. J.* **2003**, *84*, 3636–3645.
(67) Patra, M.; Karttunen, M.; Hyvönen, M. T.; Falck, E.; Vattulainen, I. *J. Phys. Chem. B* **2004**, *108*, 4485–4494.
(68) Biological Physics & Soft Condensed Matter Group of Prof. Mikko Karttunen, Dept. of Applied Mathematics, University of Western Ontario, SoftSimu - Downloads Zone. http://www.apmaths.uwo.ca/~mkarttu/downloads.shtml, File: dppc-128−100.pdb (accessed Jan 2009).
(69) Frisch, M. J.; Trucks, G. W.; Schlegel, H. B.; Scuseria, G. E.; Robb, M. A.; Cheeseman, J. R.; Vreven, T.; Kudin, K. N.; Burant, J. C.; Millam, J. M.; Iyengar, S. S.; Tomasi, J.; Barone, V.; Mennucci, B.; Cossi, M.; Scalmani, G.; Rega, N.; Petersson, G. A.; Nakatsuji, H.; Hada, M.; Ehara, M.; Toyota, K.; Fukuda, R.; Hasegawa, J.; Ishida, M.; Nakajima, T.; Honda, Y.; Kitao, O.; Nakai, H.; Klene, M.; Li, X.; Knox, J. E.; Hratchian, H. P.; Cross, J. B.; Adamo, C.; Jaramillo, J.; Gomperts, R.;

Stratmann, R. E.; Yazyev, O.; Austin, A. J.; Cammi, R.; Pomelli, C.; Ochterski, J. W.; Ayala, P. Y.; Morokuma, K.; Voth, G. A.; Salvador, P.; Dannenberg, J. J.; Zakrzewski, V. G.; Dapprich, S.; Daniels, A. D.; Strain, M. C.; Farkas, O.; Malick, D. K.; Rabuck, A. D.; Raghavachari, K.; Foresman, J. B.; Ortiz, J. V.; Cui, Q.; Baboul, A. G.; Clifford, S.; Cioslowski, J.; Stefanov, B. B.; Liu, G.; Liashenko, A.; Piskorz, P.; Komaromi, I.; Martin, R. L.; Fox, D. J.; Keith, T.; Al-Laham, M. A.; Peng, C. Y.; Nanayakkara, A.; Challacombe, M.; Gill, P. M. W.; Johnson, B.; Chen, W.; Wong, M. W.; Gonzalez, C.; Pople, J. A. *Gaussian 03*, Revision B.02; Gaussian, Inc.: Pittsburgh, PA, 2003.

(70) Schuttelkopf, A. W.; van Aalten, D. M. *Acta Crystallogr., Sect. D* **2004**, *60*, 1355–1363.

(71) Lavie, G.; Mazur, Y.; Lavie, D.; Prince, A. M.; Pascual, D.; Liebes, L.; Levin, B.; Meruelo, D. *Transfusion* **1995**, *35*, 392–400.

(72) Berendsen, H. J. C.; Postma, J. P. M.; van Gunsteren, W. F.; Hermans, J. In *Intermolecular Forces*; Reidel Publishing Company: Dordrecht, The Netherlands, 1981.

(73) Nose, S. *Mol. Phys.* **1984**, *52*, 255–268.

(74) Hoover, W. G. *Phys. Rev.* **1985**, *31*, 1695–1697.

(75) Parrinello, M.; Rahman, A. *J. Appl. Phys.* **1981**, *52*, 7182–7190.

(76) Nose, S.; Klein, M. L. *Phys. Rev. Lett.* **1983**, *50*, 1207–1210.

(77) Darden, T.; York, D.; Pedersen, L. *J. Chem. Phys.* **1993**, *98*, 10089–10092.

(78) Essmann, U.; Perera, L.; Berkowitz, M. L.; Darden, T.; Lee, H.; Pedersen, L. G. *J. Chem. Phys.* **1995**, *103*, 8577–8593.

(79) Hess, B.; Bekker, H.; Berendsen, H. J. C.; Fraaije, J. *J. Comput. Chem.* **1997**, *18*, 1463–1472.

(80) Ryckaert, J. P.; Ciccotti, G.; Berendsen, H. J. C. *J. Comput. Phys.* **1977**, *23*, 327–341.

(81) Marrink, S. J.; Berendsen, H. J. C. *J. Phys. Chem.* **1994**, *98*, 4155–4168.

(82) Steck, T. L.; Ye, J.; Lange, Y. *Biophys. J.* **2002**, *83*, 2118–2125.

(83) Bennett, W. F. D.; MacCallum, J. L.; Hinner, M. J.; Marrink, S. J.; Tieleman, D. P. *J. Am. Chem. Soc.* **2009**, *131*, 12714–12720.

(84) Jo, S.; Rui, H. A.; Lim, J. B.; Klauda, J. B.; Im, W. *J. Phys. Chem. B* **2010**, *114*, 13342–13348.

(85) Róg, T.; Stimson, L. M.; Pasenkiewicz-Gierula, M.; Vattulainen, I.; Karttunen, M. *J. Phys. Chem. B* **2008**, *112*, 1946–1952.

(86) Engelman, D. M.; Rothman, J. E. *J. Biol. Chem.* **1972**, *247*, 3694–3697.

(87) Smondyrev, A. M.; Berkowitz, M. L. *J. Comput. Chem.* **1999**, *20*, 531–545.

(88) dos Santos, D. J. V. A.; Eriksson, L. A. *Biophys. J.* **2006**, *91*, 2464–2474.

(89) Erdtman, E.; dos Santos, D. J. V. A.; Löfgren, L.; Eriksson, L. A. *Chem. Phys. Lett.* **2008**, *463*, 178–182.

(90) Burel, L.; Jardon, P. *J. Chim. Phys. Phys.* **1996**, *93*, 300–316.

(91) Falk, H.; Meyer, J. *Monatsh. Chem.* **1994**, *125*, 753–762.

(92) Allen, M. P.; Tildesley, D. J. *Computer Simulation of Liquids*; Oxford University Press: Oxford, U. K., 1990.

(93) Paci, E.; Ciccotti, G.; Ferrario, M.; Kapral, R. *Chem. Phys. Lett.* **1991**, *176*, 581–587.

(94) Bemporad, D.; Essex, J. W.; Luttmann, C. *J. Phys. Chem. B* **2004**, *108*, 4875–4884.